Phase Transitions
Publication details, including instructions for authors and subscription information:
http://www.tandfonline.com/loi/gpht20

The structure and ferroelastic phase transition of $BiVO_4$

W. I. F. David [a] , A. M. Glazer [a] & A. W. Hewat [b]
[a] Clarendon Laboratory, Parks Road, Oxford, 0X1 3PU, U.K.
[b] Institut Laue-Langevin, 156 X Centre de Tri, 38042, Grenoble, France

Available online: 19 Aug 2006

To cite this article: W. I. F. David, A. M. Glazer & A. W. Hewat (1979): The structure and ferroelastic phase transition of $BiVO_4$, Phase Transitions, 1:2, 155-169

To link to this article: http://dx.doi.org/10.1080/01411597908213198

Phase Transitions, 1979, Vol. 1, pp. 155–170
0141–1594/79/0102–0155$04.50/0

Printed in Great Britain

The Structure and Ferroelastic Phase Transition of $BiVO_4$

W. I. F. DAVID and A. M. GLAZER
Clarendon Laboratory, Parks Road, Oxford OX1 3PU, U.K.

and

A. W. HEWAT
Institut Laue-Langevin, 156 X Centre de Tri, 38042 Grenoble, France

(*Received March 3, 1979; in final form June 16, 1979*)

The structure of $BiVO_4$ has been determined by the Rietveld method at 300, 573 and 898 K and confirms the space group of the ferroelastic phase as $I2/a$ and that of the paraelastic phase as $I4_1/a$. The displacement vectors of the atoms involved in the switching of ferroelastic states are calculated and indicate that the Bi displacements are the controlling factors in the process. An analysis is given of the eigenvectors of the B_g mode responsible for the transition.

1 INTRODUCTION

Monoclinic $BiVO_4$ has been observed to undergo a ferroelastic phase transition at around 530 K to a tetragonal phase by Bierlein and Sleight (1975). These authors found that the structure of the ferroelastic phase belonged to space group $I2/a$ and they proposed that in the paraelastic phase it was $I4/a$. Raman work (Pinczuk, Burns and Dacol, 1977) strengthened the case for a ferroelastic transition of the form 4/mF2/m in Aizu's terminology (Aizu, 1969). In this work, a temperature-dependent soft optic mode was detected, whose symmetry (B_g) was the same as the strain in the $k = 0$ soft acoustic mode expected at this transition (Aubry and Pick, 1971).

In the present paper, we report on the structures of $BiVO_4$ at 300, 573 and 898 K, determined by powder neutron diffraction, and we confirm the space groups proposed by Bierlein and Sleight. Neutron diffraction was preferred to X-ray diffraction because of the greater sensitivity of neutrons to the

oxygen atoms (bismuth and oxygen have similar neutron scattering lengths, 0.860 and 0.580 $\times$ 10^{-12} cm respectively). The only disadvantage with the use of neutron diffraction in the particular case of $BiVO_4$ is that vanadium nuclei are almost transparent to neutrons (scattering length = -0.05 $\times$ 10^{-12} cm). As will be seen though, careful refinement gave sensible vanadium parameters. Powder diffraction was used as, although large crystals could be obtained, the high degree of twinning in $BiVO_4$ makes single-crystal work difficult.

2 EXPERIMENTAL PROCEDURE

The powder data were collected at 300, 573 and 898 K on the DIA diffractometer at the I.L.L. (Grenoble). The angular range was $2\theta = 0°$ to 160° in steps of 0.05° and the incident wavelength was 1.9063 Å.

Refinement was carried out with the Rietveld programme (Rietveld, 1969) modified by Hewat (1973). For the 300 K data, space group $I2/a$ was used, after confirming Bierlein and Sleight's assignment for ourselves with Weissenberg photographs. (In this work we use the first monoclinic setting, i.e. with 2_1 along [001], in order to compare parameters directly with the high-temperature phase). The high-temperature data were refined in $I4_1/a$. Both isotropic and anisotropic temperature factors were refined.

3 PARAELASTIC PHASE

Figure 1(a) shows the observed and calculated profiles at 898 K. It can be seen that an excellent fit has been established. Table I gives the resulting parameters at 573 and 898 K. It is interesting to note that, despite the near transparency of the V atoms to neutrons, anisotropic temperature factors could be refined and even gave magnitudes which seemed reasonable. In addition, all the temperature factors for the 898 K data are larger than for the 573 K data, as would be expected, thus supporting the idea that the temperature factors obtained are not spurious. The very low R-factors also are strong evidence that the structural model gives an excellent fit to the data and that, therefore, the assignment of space group $I4_1/a$ is undoubtedly correct.

The structure is of the undistorted scheelite type, Figure 2. This consists of isolated VO_4 tetrahedra, which are slightly elongated along the $\bar{4}$ axis and have $\bar{4}2m$ symmetry. The V—O bond lengths (Table III), 1.733 Å at 898 K, are in close agreement with the predictions of Shannon and Prewitt (1969),

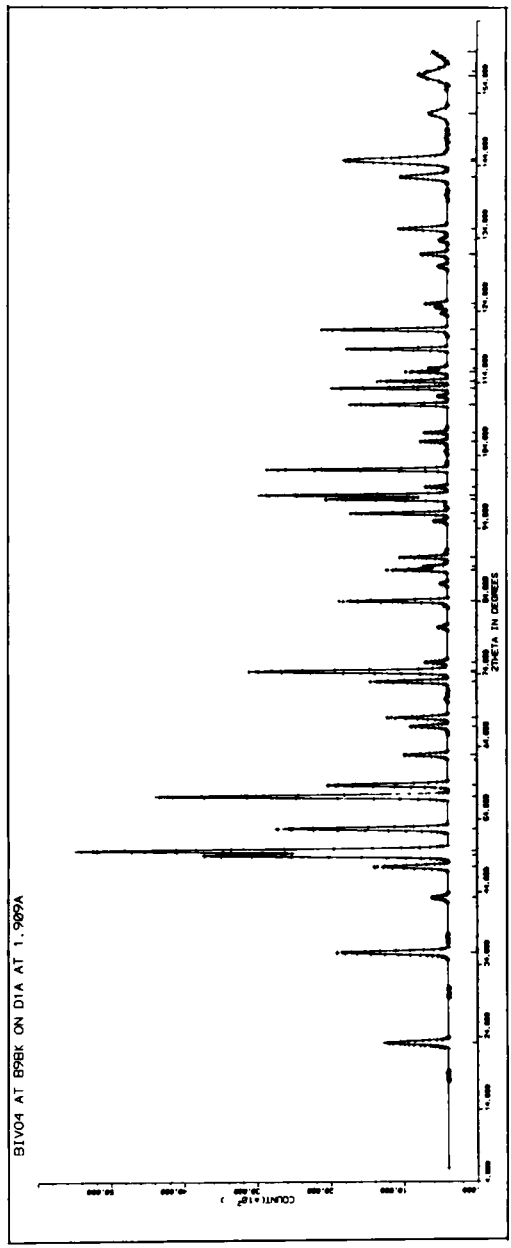

FIGURE 1a Observed and calculated neutron diffraction profiles of $BiVO_4$ at 898 K.

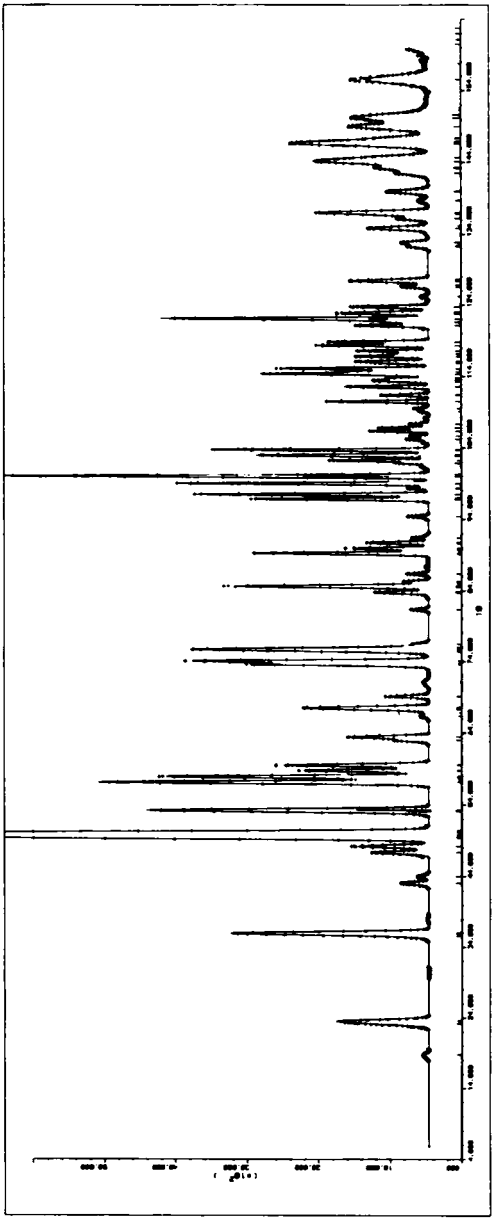

FIGURE 1b Observed and calculated neutron diffraction profiles of $BiVO_4$ at 300 K.

TABLE I

$BiVO_4$ structural parameters at 573 K and 898 K Space group $I4_1/a$

Bi at 0, 0, $\frac{1}{2}$ and V at 0, 0, 0

573 K Refinement

a = 5.1509(5) Å c = 11.730(1) Å

R_{INT} = 2.72% R_{PROF} = 5.93%

	x	y	z
O	0.2491(2)	0.1379(2)	0.0782(1)

	B_{11}	B_{22}	B_{33}	B_{12}	B_{13}	B_{23}	(Å^2)
Bi	1.46(3)	1.46(3)	1.97(6)	—	—	—	
V	0.8(5)	0.8(5)	1.2(7)	—	—	—	
O	1.71(4)	1.64(4)	1.68(4)	−0.24(4)	−0.44(4)	0.23(3)	

898 K Refinement

a = 5.1724(5) Å c = 11.809(1) Å

R_{INT} = 3.64% R_{PROF} = 6.74%

	x	y	z
O	0.2491(2)	0.1364(2)	0.0779(1)

	B_{11}	B_{22}	B_{33}	B_{12}	B_{13}	B_{23}	(Å^2)
Bi	2.18(4)	2.18(4)	3.08(7)	—	—	—	
V	1.1(5)	1.1(5)	1.3(8)	—	—	—	
O	2.66(4)	2.51(4)	2.75(4)	−0.48(5)	−0.63(5)	0.28(4)	

$B_{ij} = 8\pi^2$ [mean square amplitude]^2 in Å^2

R_{INT} and R_{PROF} are as defined by Rietveld (1969).

indicating that the V atom is fairly rigidly held within the oxygen tetrahedron. The Bi atoms are situated midway between the tetrahedra and are coordinated to eight O atoms. Figure 3 shows the (001) projection at 898 K. At 573 K the projection is almost identical, with the thermal ellipsoids in the same orientation, but with smaller magnitudes. The shapes and orientations of the ellipsoids seem to indicate that the VO_4 tetrahedra are rigidly oscillating about [001] and that this is coupled with a small distortional mode of the tetrahedra. For the Bi atoms, $B_{33} > B_{11} = B_{22}$ and this suggests that these atoms exhibit large-amplitude motion along [001].

4 FERROELASTIC PHASE

Below 530 K the $\bar{4}$ and 4_1 symmetry elements of the paraelastic phase are lost and the crystal changes from tetragonal to monoclinic symmetry.

Table II lists the refined parameters, both with isotropic and anisotropic temperature factors. The positional parameters are essentially the same in

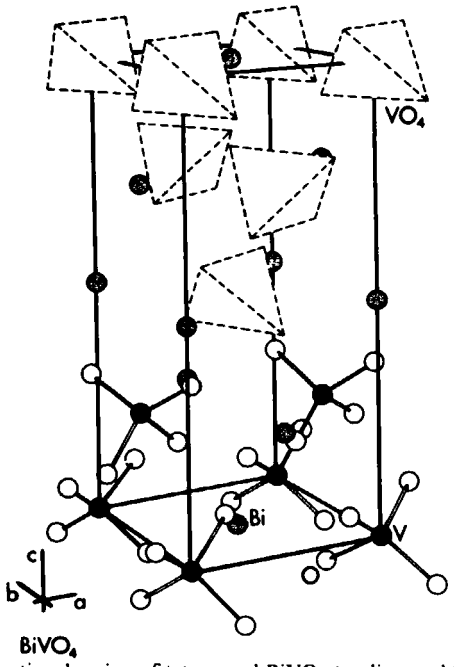

FIGURE 2 Perspective drawing of tetragonal $BiVO_4$ (undistorted Scheelite structure).

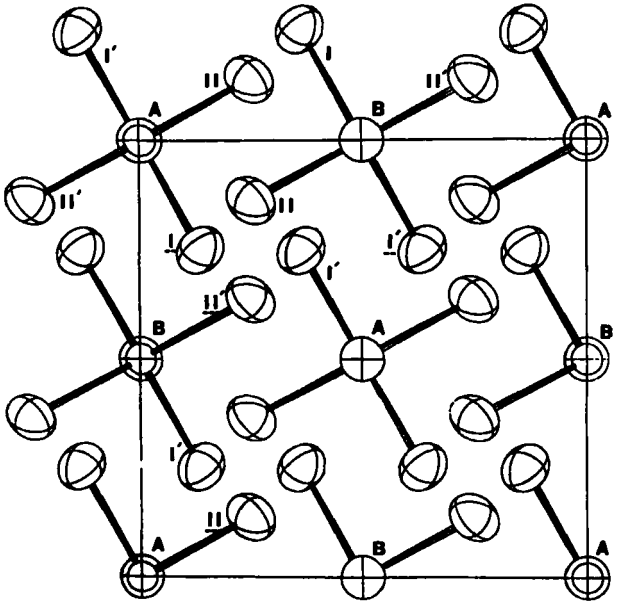

FIGURE 3 (001) projection of $BiVO_4$ at 898 K. Tetrahedra labelled A are linked to one another by body-centring. (Tetrahedra labelled B are similarly linked to one another.) In $I2/a$ all O atoms labelled I are symmetry-related to one another. Similarly for O atoms labelled II. In $I4_1/a$ all O atoms are symmetry-related.

TABLE II

$BiVO_4$ structural parameters at 300 K. Space group $I2/a$

(a) Isotropic temperature factor refinement

$a = 5.1966(5)$ Å $b = 5.0921(5)$ Å $c = 11.704(1)$ Å $\gamma = 89.616(1)°$

$R_{INT} = 4.05\%$ $R_{PROF} = 6.06\%$

atom	x	y	z	B (Å^2)
Bi	0	0	0.4192(1)	0.76(2)
V	0	0	−0.0025(15)	0.81(20)
O1	0.2395(2)	0.1314(2)	0.0740(1)	0.96(2)
O2	−0.1477(2)	0.2586(2)	−0.0836(1)	0.78(2)

(b) Anisotropic temperature factor refinement

$R_{INT} = 3.98\%$ $R_{PROF} = 5.79\%$

atom	x	y	z
Bi	0	0	0.4911(1)
V	0	0	−0.0006(15)
O1	0.2396(2)	0.1310(2)	0.0741(1)
O2	−0.1478(2)	0.2584(2)	−0.0836(1)

	B_{11}	B_{22}	B_{33}	B_{12}	B_{13}	B_{23}
Bi	0.80(3)	0.66(4)	0.83(4)	0.03(3)	—	—
V	2.1(7)	−0.9(6)	1.8(7)	—	—	—
O1	0.86(4)	0.98(4)	1.14(5)	−0.06(3)	−0.18(4)	0.01(3)
O2	0.72(4)	0.68(4)	1.02(5)	0.19(3)	0.07(3)	0.33(4)

$B_{ij} = 8\pi^2$ [mean square amplitude]^2 in Å^2

both cases, the small difference in the V coordinates being less than the statistical uncertainty. The main differences between this structure and that of the paraelastic phase are

1) all the atoms are displaced along [001] and [00$\bar{1}$] in alternating (001) layers (see Figure 4(a)), the largest displacements being those of the Bi atoms.

2) the tetrahedra are distorted as indicated in Figure 4(b). For example, the tetrahedron at the origin has the two O atoms at the top further apart than those on the bottom, to give one long O—O distance and one short one.

The distortional change can also be seen in Table III, where the bond lengths are given. As is seen, the bond lengths of the paraelastic phase lie precisely between pairs of bond lengths in the 300 K structure, thus showing that the monoclinic phase involves a small distortion of the tetragonal phase, consistent with the ferroelastic transition. This also implies that the structure

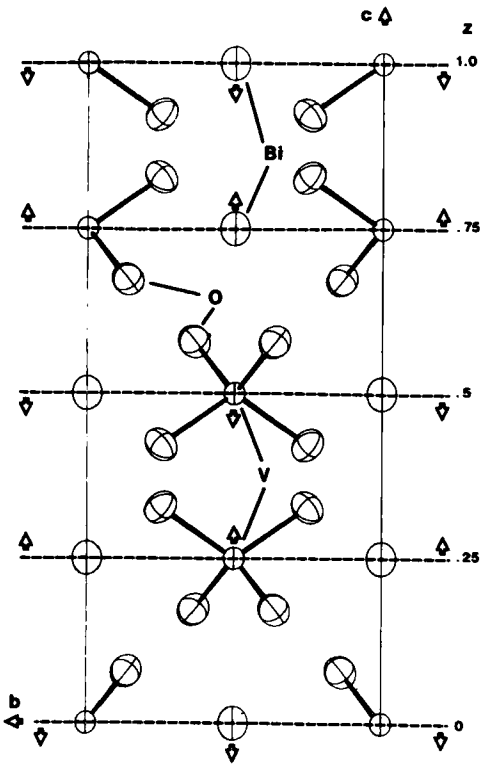

FIGURE 4a Atom displacement along [001] and [00$\bar{1}$] in ferroelastic phase (with respect to paraelastic phase).

TABLE III

Bond lengths in Å
(See Figure 3 for labelling of atoms)

	Temperature		
	300 K	573 K	898 K
V – OI	1.670	1.730	1.733
V – OII	1.792		
OI – OII	2.809	2.769	2.776
OI – OII′	2.750		
OI – OI′	2.818	2.933	2.938
OII – OII′	3.039		
Bi – OI	2.5020	2.448	2.463
Bi – OII	2.3789		
Bi – OI′	2.6404	2.497	2.513
Bi – OII′	2.3431		

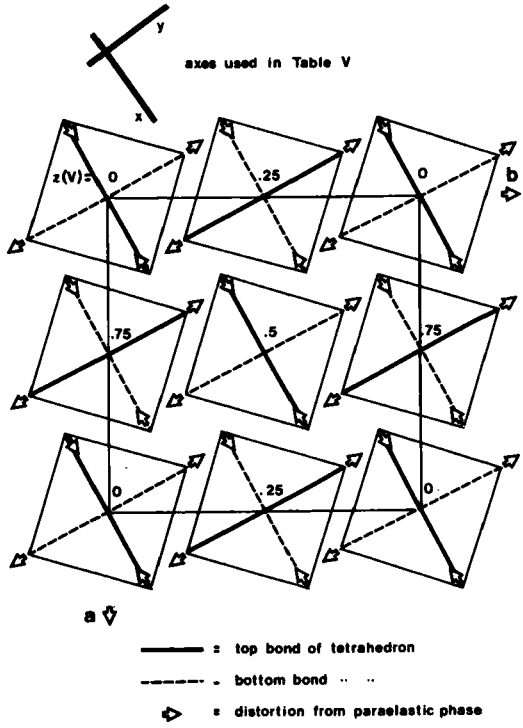

FIGURE 4b Atom displacements in (001) plane in ferroelastic phase (with respect to paraelastic phase).

of the paraelastic phase lies midway between the two permissible ferroelastic orientation states, a typical condition for ferroelastic switching. Using this idea and the definition given by Aizu (1970), we calculate the spontaneous strain to be 15×10^{-3}, about one half that of the well-known ferroelastic $Pb_3(PO_4)_2$ (Guimaraes, 1979).

In a full ferroelastic species such as this it is worth considering what happens to the atoms during the ferroelastic switching process. In $BiVO_4$ the ferroelastic orientation states are related by a pseudo 4_1 axis. In order to calculate the relative displacements of the atoms we use the method of Guimaraes (1979) where a rotation is applied to the coordinates of the atoms in orientation state 1 and the resulting positions are compared with other atoms in the same orientation state. The difference between these positions gives the displacement magnitudes Δ of the atoms during the switching process. Symbolically this is

$$\Delta = R x_i - x_j$$

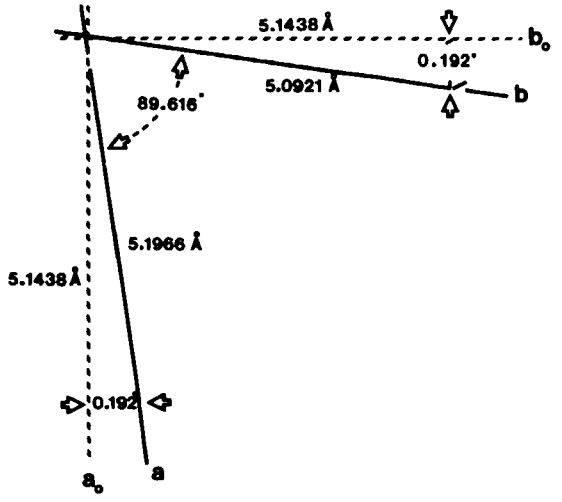

FIGURE 5 Relationship between hypothetical 300 K prototypic tetragonal cell and 300 K monoclinic cell ($c_{\text{tetragonal}} = c_{\text{monoclinic}}$).

where R is the rotation operation, x_i represents the orthogonal Ångstrom coordinates of atom i in state 1 and x_j those of atom j in the same state. In the present case, we take our origin on the 4_1 axis so that the pseudo-operation applied is actually a 4_1 screw axis. In order to obtain orthogonal Ångstrom coordinates we choose new axes a_o, $b_o(a_o = b_o)$ as in Figure 5; these correspond to a hypothetical prototype (paraelastic) phase at room-temperature at the mid-position of the ferroelastic switching. During this process, with reference to orientation state 1 (ferroelastic domain 1), a must shorten, b must increase and γ must become obtuse to produce orientation 2 (domain 2), in which the unit cell appears to have rotated through 90° about [001]. Table IV gives the displacements calculated in this way, Δ_{xy}

TABLE IV

Displacements (in Å) of atoms during switching at room temperature

	Rx_1	Ry_1	Rz_1	x_2	y_2	z_2	Δ_{xy}	Δ_z	$\lvert\Delta\rvert$
Bi	−1.2773	1.3035	8.6747	−1.2948	1.2687	8.8815	0.039	−0.207	0.210
V	−1.2773	1.3035	2.897	−1.2948	1.2687	2.955	0.039	−0.06	0.07
01	−0.6050	0.0565	3.7927	−0.5317	−0.0451	3.9041	0.125	−0.111	0.168
02	0.5317	0.0451	3.9041	0.6050	−0.0565	3.7927	−0.125	0.111	0.168

R is the 4_1 operation $\Delta_{xy} = [(Rx_1 - x_2)^2 + (Ry_1 - y_2)^2]^{1/2}$

$\Delta_z = Rz_1 - z_2$

$\Delta = (\Delta_{xy}^2 + \Delta_z^2)^{1/2}$

All coordinates are referred to the constructed tetragonal axes a_0, b_0 shown in Figure 5.

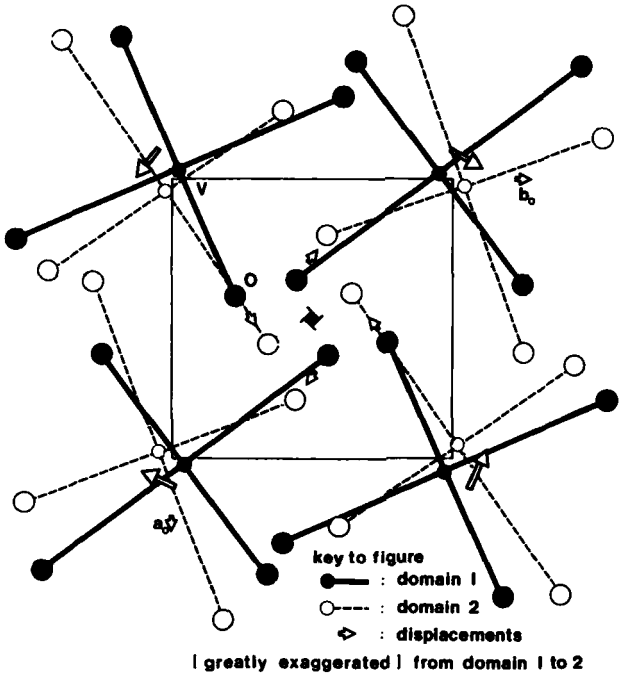

FIGURE 6 Relationship between the two ferroelastic orientation states.

being the displacements in the (001) plane, Δ_z those along [001] and Δ the total resultant displacement. The V displacements are small and, given the large standard deviations of the z coordinates, are not significant. We see that the largest overall displacement is to the Bi atom, principally in the [001] direction, the effect of switching being essentially to change the Bi z parameter from being above the prototypic value to below it. The oxygen displacements are also quite large (approximately 0.17 Å overall) but in this case there is also a large contribution from movement in the (001) plane ($\pm$0.125 Å). The latter effect is schematically shown in Figure 6 where it is seen that this produces a switching of the tetrahedral distortion shown in Figure 4(b) with the long O—O distances contracting and the short ones expanding. The [001] displacement means that the whole tetrahedron is displaced in the same way as the Bi atom.

We can explain the negligible V displacement as follows. The O tetrahedron is distorted as shown, with the V atom occupying a position closer to the longer O—O bond. During switching the contraction of this bond and expansion of the shorter one means that the V atom would become closer to the O atoms unless the V atom or the tetrahedron is displaced also along [001]. However because of the Bi displacements the major effect is on the

oxygen atoms towards which the Bi atom moves and so it is the displacement along [001] of the O tetrahedron that predominates over the V displacement. Such a model suggests that the displacement of the Bi atom is the major controlling factor in the switching process with the O tetrahedron displacements as secondary. This view is supported by the fact that Δ_z for Bi (see Table IV) is considerably larger than for O. Similar behaviour is found in the improper ferroelastic $Pb_3(PO_4)_2$ (Guimaraes, 1979) where the Pb atoms seem to play the major role (in this case the evidence came from considering the Δ's as a function of temperature). It is tempting to suggest that *in ferroelastics there will in general be a particular atom (or group of atoms) which controls the switching capability with all other atomic displacements following as a consequence.* This is analogous to the case of ferroelectrics, where it is known that the spontaneous polarization is connected closely with a small group of atoms, as in perovskites where the B cation usually plays an important part. Further studies of ferroelastic structures will be needed to see if this is indeed a general principle. It would be of particular interest in this connection to study the displacement vectors of the atoms in $BiVO_4$ as a function of temperature in order to correlate them with the spontaneous strain. It is worth pointing out that in both $Pb_3(PO_4)_2$ and $BiVO_4$ the controlling ion has a lone electron pair, and it is presumably this that is responsible for making such an ion play the major role in the ferroelastic behaviour.

5 THE FERROELASTIC-PARAELASTIC TRANSITION

According to Aubry and Pick (1969) for the ferroelastic species 4/mF2/m the strain associated with the acoustic mode responsible for the transition to the ferroelastic phase must have B_g symmetry. As mentioned earlier, Raman scattering studies showed that there was a soft-optic mode of B_g symmetry in $BiVO_4$ and that, therefore, there is a strong coupling between the acoustic and optic modes. We can use our structure determination to suggest the eigenvectors of the relevant B_g modes by using standard group-theoretical techniques. Treating the atoms separately, we find for $k = 0$ the following irreducible representations

$$\Gamma(\text{Bi}) = 2B_g + 2E_g + 2A_u + 2E_u$$

$$\Gamma(\text{V}) = 2B_g + 2E_g + 2A_u + 2E_u$$

$$\Gamma(\text{O}) = 6A_g + 6B_g + 3E_g + 6A_u + 6B_u + 3E_u$$

and so we see that all atoms are potentially involved in the B_g modes in question.

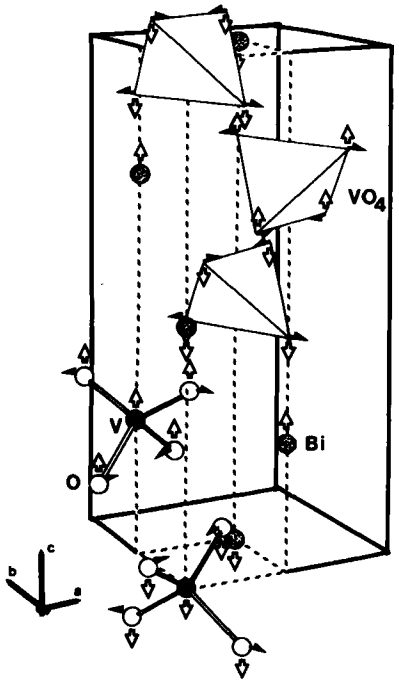

FIGURE 7 Ferroelastic structural distortion from paraelastic structure. The two B_g modes are shown by the light and dark arrows.

Applying character projection-operator methods we find the relationships between the component displacements shown in Table V. This pattern of displacements, of course, corresponds to a superposition of all ten B_g modes, as group-theoretical techniques alone cannot separate symmetry-equivalent species. Therefore in order to identify the soft-mode eigenvectors we must take into account the structure that we have determined for the ferroelastic phase. From this we see that the structural distortion from the paraelastic structure can be represented as in Figure 7, and this is entirely consistent with the relationships of Table V (see Figure 4(b)). This in itself is a superposition of two B_g modes, both optic, and it is a straightforward matter to identify the component eigenvectors. One B_g mode must involve antiphase motion, in this case, of alternate (001) layers moving along [001] and [001] (see Figures 4(a) and 7). The other can be identified as the stretching and contraction of the O—O bonds of the tetrahedra within the (001) planes, clearly related to the spontaneous strain tensor (Aizu, 1970) which only contains terms relevant to (001). We can also see from our structural

TABLE V

Acoustic and optic mode component displacements using projection operators

Symmetry elements of point group 4/m	1	4	2	4^3	$\bar{1}$	$\bar{4}$	m	$\bar{4}^3$
Equivalent elements of $14_1/a$ ($\{R\|0\}$)	1	4_3^*	4_3^3	4_3^2	$\bar{1}$	$\bar{4}$	a	$\bar{4}^3$
Characters of B_g (χ)	1	−1	1	−1	1	−1	1	−1
$\chi R(-x_{IA})$	$-x_{IA}$	$-(-y_{IIB})$	$x_{I'A}$	$-(-y_{II'B})$	x_{IB}	$-(y_{IIA})$	$-x_{I'B}$	$-(-y_{II'A})$
$\chi R(-z_{IA})$	$-z_{IA}$	$-(-z_{IIB})$	$-z_{I'A}$	$-(-z_{II'B})$	z_{IB}	$-(z_{IIA})$	$z_{I'B}$	$-(z_{II'A})$
$\chi R(-z_{00\frac{1}{2}})$	$-z_{00\frac{1}{2}}$	$-(-z_{\frac{1}{2}0\frac{1}{4}})$ $\equiv z_{0\frac{1}{2}\frac{1}{4}}$	$-z_{\frac{1}{2}\frac{1}{2}0}$ $\equiv -z_{00\frac{1}{2}}$	$-(-z_{0\frac{1}{2}\frac{1}{4}})$	$-z_{0\frac{1}{2}\frac{1}{4}}$	$-(z_{00\frac{1}{2}})$	$z_{\frac{1}{2}0\frac{1}{4}}$ $\equiv z_{0\frac{1}{2}\frac{1}{4}}$	$-(z_{00\frac{1}{2}})$
$\chi R(-z_{000})$	z_{000}	$-(-z_{\frac{1}{2}0\frac{1}{4}})$	$-z_{\frac{1}{2}\frac{1}{2}\frac{1}{4}}$ $\equiv -z_{000}$	$-(-z_{0\frac{1}{2}\frac{1}{4}})$ $\equiv z_{\frac{1}{2}0\frac{1}{4}}$	$z_{0\frac{1}{2}\frac{1}{4}}$ $\equiv z_{\frac{1}{2}0\frac{1}{4}}$	$-(z_{000})$	$z_{\frac{1}{2}0\frac{1}{4}}$	$-(z_{000})$

Oxygen atoms (a) Optic mode distortion $= (x_{I'A} - x_{IA} + y_{II'A} - y_{II'B}) + (x_{IB} - x_{I'B} + y_{IIB} - y_{II'B})$

(b) Optic mode distortion $= (z_{IA} + z_{IIA} + z_{I'A} + z_{II'A}) + (z_{IB} + z_{IIB} + z_{I'B} + z_{IIB})$

Bismuth atom Optic mode distortion $= -z_{00\frac{1}{2}} + z_{0\frac{1}{2}\frac{1}{4}}$

Vanadium atom Optic mode distortion $= -z_{000} + z_{\frac{1}{2}0\frac{1}{4}}$

* 4_3 is along [001] through $(\frac{1}{4}, \frac{1}{4}, 0)$ and $(\frac{3}{4}, \frac{3}{4}, 0)$ or 4_1 along [001] through $(\frac{1}{4}, \frac{3}{4}, 0)$ and $(\frac{3}{4}, \frac{1}{4}, 0)$

model that the two B_g modes are strongly coupled. As described earlier the vibration of the Bi atoms along [100] must cause a similar movement, for steric reasons, to the oxygen tetrahedron. This in turn causes a distortion in the (001) plane of the tetrahedron as it moves against the V atom. The coupling may therefore be so strong that the motion can be described as a single B_g optic mode.

Acknowledgements

We wish to thank the Institute Laue-Langevin for access to the neutron and computing facilities, and the Science Research Council for a C.A.S.E. award.

References

Aizu, K. (1969). Possible species of 'ferroelastic' crystals and of simultaneously ferroelectric and ferroelastic crystals. *J. Phys. Soc. Japan*, **27**, 387.

Aizu, K. (1970). Determination of the state parameters and formulation of spontaneous strain for ferroelastics. *J. Phys. Soc. Japan*, **28**, 706.

Aubry, S. and R. Pick (1971). Soft-modes in displacive transitions. *J. de Physique*, **32**, 657.

Bierlein, J. D. and A. W. Sleight (1975). Ferroelasticity in $BiVO_4$. *Solid State Commun.*, **16**, 69.

Guimaraes, D. M. C. (1979). Ferroelastic transformations in lead orthophosphate and its structure as a function of temperature. *Acta Cryst.*, **A35**, 108.

Hewat, A. W. (1973). Cubic-tetragonal-orthorhombic-rhombohedral ferroelectric transitions in perovskite potassium niobate: neutron profile refinement of the structures. *J. Phys. C*, **6**, 2559.

Pinczuk, A., G. Burns, and F. H. Dacol (1977). Soft optical phonon in ferroelastic $BiVO_4$. *Solid State Commun.*, **24**, 163.

Rietveld, H. M. (1969). A profile refinement method for nuclear and magnetic structures. *J. Appl. Cryst.*, **2**, 65.

Shannon, R. D. and C. T. Prewitt (1969). Effective ionic radii in oxides and fluorides. *Acta. Cryst.*, **B25**, 925.